Available online at www.sciencedirect.com
SCIENCE DIRECT
Journal of Molecular Graphics and Modelling 24 (2006) 319–327
Journal of Molecular Graphics and Modelling
www.elsevier.com/locate/JMGM

Homology modelling and protein structure based functional analysis of five cucumovirus coat proteins

Ákos Gellért [a,b,*], Katalin Salánki [a], Gábor Náray-Szabó [c], Ervin Balázs [a,d]

[a] *Agricultural Biotechnology Center, Szent-Györgyi Albert u. 4, H-2100 Gödöllő, Hungary*
[b] *Department of Theoretical Chemistry, Eötvös Loránd University, Pázmány Péter stny. 1/A, H-1117 Budapest, Hungary*
[c] *Protein Modelling Group, Hungarian Academy of Sciences and Eötvös Loránd University, Pázmány Péter stny. 1/A, H-1117 Budapest, Hungary*
[d] *Agricultural Research Institute of the Hungarian Academy of Sciences, Brunszvik u. 2, H-2462 Martonvásár, Hungary*

Received 5 January 2005; received in revised form 14 July 2005; accepted 29 September 2005
Available online 28 October 2005

Abstract

Coat proteins (CP) of five cucumovirus isolates, Cucumber mosaic virus (CMV) strains R, M and Trk7, Tomato aspermy virus (TAV) strain P and Peanut stunt virus (PSV) strain Er, were constructed by homology modelling. The X-ray structure of the Fny-CMV CP subunit B was used as a template. Models of cucumovirus CPs were built by the MODELLER program. Model refinements were carried out using the Kollman molecular mechanical force field. Models were analyzed by the PROCHECK programs. Electrostatic potential calculations were applied to all models and functional site search was performed with the PROSITE software, a web based tool for searching biologically significant sites. Symptom determinants published up to the present were compared with the PROSITE hits in the light of 3D models and electrostatic information. In all cases, we analyzed the effect of mutations on the structure, electrostatic potential patterns and function of CPs, respectively. We found that high flexibility of the βE–αEF loop starting with the residue 129 is required, but it is not sufficient for the symptom appearance. Furthermore, phosphorylation of the CP is prospective to be important in the host response mechanism. All analyzed mutations were related to the modifications of the predicted phosphorylation sites. Based on our conclusions we predicted the infectivity of the examined viruses.

Keywords: Homology modelling; Sequence analysis; Electrostatic potential analysis; Virology; Phosphorylation

1. Introduction

Cucumoviruses infect over 1000 plant species and cause considerable harm to agriculture worldwide, therefore understanding the molecular mechanism of the virus spread is of utmost importance. *Cucumber mosaic virus* (CMV), *Tomato aspermy virus* (TAV) and *Peanut stunt virus* (PSV) form the *Cucumovirus* genus in the family Bromoviridae. Their genomes consist of three single-stranded, positive-sense RNA molecules. The RNA 3 encodes two proteins, the movement protein (MP) and the coat protein (CP). The main function of the CPs is to encapsulate the viral RNAs. The virus particle is composed of 180 CPs with a $T = 3$ truncated icosahedral symmetry [1].

In addition, the CP plays significant role in the infection process. The capsid protein is indispensable for cell-to-cell and long distance movement of the virus within plants, and also between plants since it contains determinants for aphid transmission [2]. Besides the movement protein the cucumoviruses also require the CP for cell-to-cell movement [3], but the assembly of the virus particle is not required [4]. If the C-terminal 33 amino acids (aa) were deleted from the MP, the CP was not necessary for the cell-to-cell movement of CMV [5]. In a previously published study [6], we showed that these viral proteins are not reversely exchangeable between R-CMV and P-TAV. The CP structure of a non-infectious chimeric virus construct was compared with a CP from an infectious construct and significant electrostatic potential pattern differences were shown. With a designed double point mutation the non-infectious construct became infectious as its electrostatic pattern mimicked the infectious one. The significance of this phenomenon is fasc-

* Corresponding author. Tel.: +36 28 526 140; fax: +36 28 526 192.
E-mail address: gellert@abc.hu (Á. Gellért).

1093-3263/$ – see front matter © 2005 Elsevier Inc. All rights reserved.
doi:10.1016/j.jmgm.2005.09.015

inating since direct interaction was not yet proved between the MP and CP [2]. However, in cucumoviruses the accurate role of the CP in the cell-to-cell movement is still unknown.

A homology model based study of *Potato leafroll virus* (PLRV) [7] was previously reported and now we present five cucumovirus CPs for which pathological features are well described. There are only two cucumovirus CPs, for which the 3D structure have been resolved, the Blencowe strain of TAV and Fny-CMV. The 3D structures of the other cucumovirus CPs can be modelled without difficulties, because their sequence similarity is very high. The following model structures were created: CP of CMV strains R, M and Trk7, P-TAV and Er-PSV CP. In the literature, there are also examples showing that the replacement of one or two residues in the CP can alter the infectivity of the virus, leading to different symptoms or a non-infectious virus becomes infectious on a special host plant [3,6,19,20,21]. These cases are analyzed in this paper and we discuss the experimental results on the basis of structural and functional aspects using spatial, electrostatic and hydrophobic determinants of the compared CPs [8]. Additionally, we make predictions for the other cucumovirus CPs. Theoretical analysis suggests that the different phosphorylation states of CPs in the host plant cell induce alternative biochemical pathways in the process of the virus infection. On the basis of this study further experiments can be designed which allow deeper understanding of the molecular mechanism of virus infection.

2. Methodology

2.1. Sequence alignment, phylogenetic analysis, homology modelling, model refinement, electrostatic calculations, structure evaluation of the CPs and PROSITE search

Sequence alignments and similarity values were calculated using the Gap program [9] of the Wisconsin Package Version 10.0 [10]. All CPs' (R, M, Trk7-CMV, P-TAV and Er-PSV) sequence analyses indicated high levels of homology. The sequences appear in the EMBL/GenBank/DDBF databases under accession numbers Y18138, AF268599, L15336, L15335 and U15730 for the R-CMV CP, M-CMV CP, Trk7-CMV CP, P-TAV CP and Er-PSV CP, respectively. Phylogenetic analysis was done by the PHYLYP 3.5 program [11] package, while the distance matrix was computed using the PROTDIST maximum likelihood based program with 100 bootstraps. Phylogeny tree searching was performed by the KITSCH program, coat protein models were constructed employing the MODELLER 6.1 program [12]. Five models have been generated using the subunit B of Fny-CMV coat protein (PDB ID code 1F15) as the template structure [1]. All models contain 190 residues from residues 29 to 218 corresponding to the B chain of the template coat protein. The models were refined with energy minimization using a molecular mechanics force field (Kollman-All-Atom with Kollman charges [13]) incorporated in the SYBYL 6.5 software package. At the beginning of the energy minimization the steepest descent technique was used to eliminate the steric conflicts between the side-chain atoms until the root mean square (rms) force was reduced to 50 kcal/(mol Å). Arriving to this threshold, the program automatically continued the energy minimization performing the Powell conjugate gradient optimization until the maximum force became less than 0.05 kcal/(mol Å). We applied a distance dependent dielectric constant ($\varepsilon = 4R$). The atomic charges for all atoms were obtained from the Kollman-All-Atom force field. Electrostatic potential maps were calculated by the linearized Poisson–Boltzmann method [14] using dielectric constant values of 80 and 4.0 for the water solvent and protein core, respectively. The ionic strength was fixed at 0.1 mol/l. All Lys (+1), Arg (+1), Glu (−1) and Asp (−1) side chains were considered as ionized (actual charges in parentheses). Atomic charges were calculated by the GRASP program [15]. Molecular graphics and the electrostatic potential representations were created by the Swiss PDB Viewer 3.7 [16] using GRASP surface files with electrostatic property. Evaluation of the refined models was carried out with PROCHECK [17] and Swiss PDB Viewer 3.7. Functional site searching was performed using PROSITE a web based tool for searching biologically significant sites [18].

3. Results and discussion

3.1. Homology modelling, phylogenetic analysis and predicted functional sites

The aa sequence alignments of the cucumovirus CPs to the B subunit of the template Fny-CMV CP are shown in Fig. 1. The percentage of the aa sequence similarities and identities are shown in Table 1. Due to the high levels of homology, gap openings and insertions were not necessary in the modelled range (residues 29–218) except the sequence of the Er-PSV. In this case, Glu-29 of the Er-PSV CP corresponds to Asn-31 of the template and residues 29–216 were modelled. The reliability of the models is demonstrated in Table 2. The models begin with residue 29, because in the B subunit of the template Fny-CMV CP residues 1–28 are disordered and could not be located by X-ray diffraction [1]. The structure of the CP is shown in Fig. 2.

The phylogenetic tree of the proteins investigated is presented in Fig. 3. Evolutionary distances show that CMV M and Fny strains are from subgroup I, while the R and Trk7-CMV belong to subgroup II, Er-PSV is the most distant from CMV.

Eight types of functional sites were found by PROSITE (Fig. 1): asparagine-glycosylation and amidation sites which

Table 1
Amino acid sequence similarities and identities of investigated CPs[a]

Protein name	Percent similarity[b]	Percent identity[b]
R-CMV CP	88.5	82.0
M-CMV CP	97.2	96.3
Trk7-CMV CP	86.6	80.6
P-TAV CP	58.1	45.2
ER-PSV CP	60.5	50.0

[a] Fny-CMV CP sequence was used as reference.
[b] Gap program was used to calculate sequence alignments. The program uses the alignment method of Needleman and Wunsch [9].

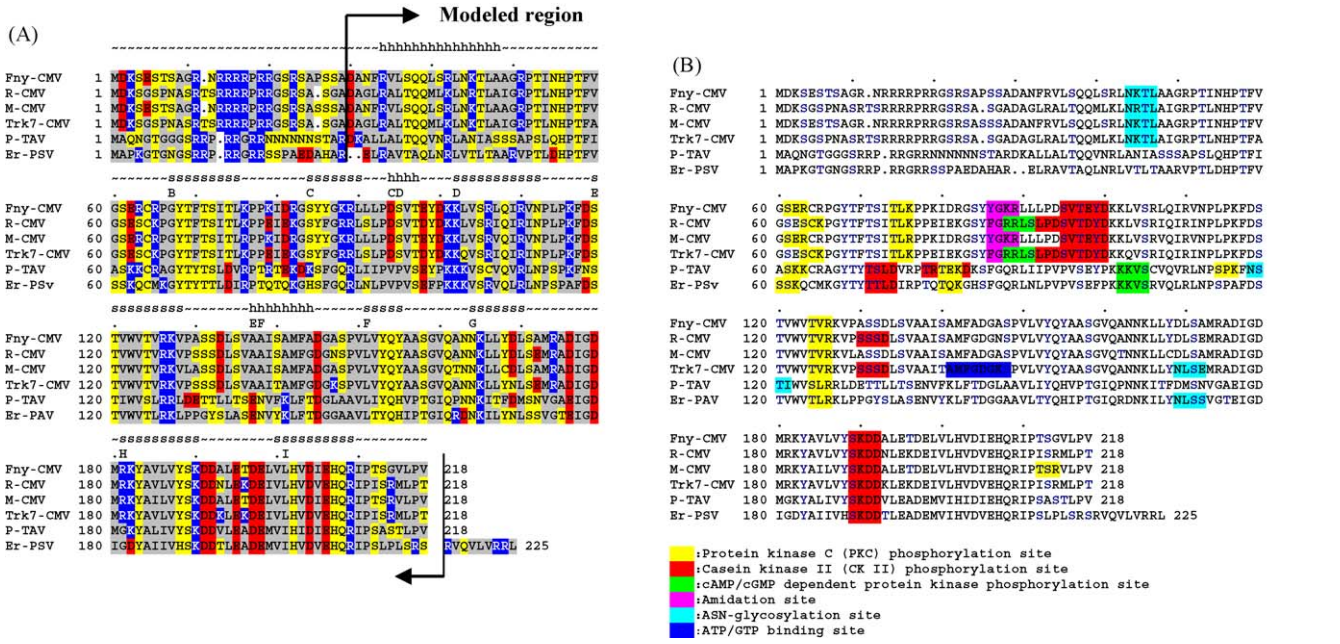

Fig. 1. Multiple sequence alignment between Fny-CMV CP and R, M, Trk7-CMV, P-TAV and Er-PSV CPs produced by the Gap program. (A) The secondary structure of CPs is shown by letters, 's' showing β-sheets and h for α-helices. The background of the sequence alignment reflects the amino acid chemical property: acidic amino acids (aas) are red, basic aas are blue, polar aas are yellow and hydrophobic aas are grey. (B) Background shading indicates important PROSITE hits. Serins, threonins and tyrosins, which can be phosphorylated, are coloured blue.

are conservative in all CMV CP sequences, cAMP/cGMP dependent protein kinase phosphorylation sites were found in two CMV CPs and ATP/GTP binding site was found in the Trk7-CMV CP. All modelled cucumovirus CPs contain conservative protein kinase C (PKC) and casein kinase II (CK II) phosphorylation sites at a few positions. There are two false hits (data not shown) which are predicted in the middle of the sequences, these are the N-terminal myristoylation and C-terminal microbody targeting signal sites. In this work, phosphorylation as a general biochemical regulation facility was used to interpret the earlier experimental results. Further experiments are required to verify other predicted functions.

3.2. Stunting determined by a single amino acid residue at position 193

R-CMV induces a very strong stunting response in *Nicotiana glutinosa* plants, while Trk7-CMV causes green mosaic in the same host plant [19]. R and Trk7-CMV CPs contain an asparagine (N) and a lysine (K) residue at position 193, respectively. Residue 193 is located at the βH–βI loop between the H and the I β-sheets, which is on the well accessible external surface of the assembled virus capsid. Both point mutations K193S and K193N in the Trk7-CMV CP induced very strong stunting in *N. glutinosa* plant [19]. Why does stunting evolve in case of the above-mentioned two mutations? Comparison of the Trk7 and R-CMV CP homology models after a PROSITE functional site search indicates that, there is a casein kinase II phosphorylation site between positions 189 and 192. Probably, the charge of the residue at position 193 influences the kinase bonding on the surface of the CP (Fig. 4). Unfortunately, on this base it cannot be decided which CP inhibits phosphorylation. Owing to the positive charge of K193 and the negatively polarized N193, different biochemical pathways are activated in the infection process. This functional site can be also phosphorylated in the

Table 2
Quality of structures refined by the SYBYL program[a]

Refined model	Ramachandran plot quality (%)			Goodness factors		rms deviation (Å) from template backbone
	Allowed	Generally allowed	Disallowed	Covalent	Total	
Fny-CMV (template)	95.2	1.8	3.0	−0.02	−0.18	–
R-CMV	98.2	0.6	1.2	0.37	−0.10	0.77
M-CMV	97.6	0.0	2.4	0.38	−0.05	0.86
Trk7-CMV	98.2	0.6	1.2	0.37	−0.08	0.77
P-TAV	98.2	0.6	1.2	0.33	−0.09	0.83
ER-PSV	98.2	0.6	1.2	0.34	−0.08	0.84

[a] Ramachandran plot qualities show the amount (%) of residues belonging to the allowed, generally allowed and disallowed region of the plot. Goodness factors show the quality of the covalent and overall bond/angle distances, these scores should be above −0.50 for reliable models. The rms deviation values indicate the overall deviation of the 3D structure from the template.

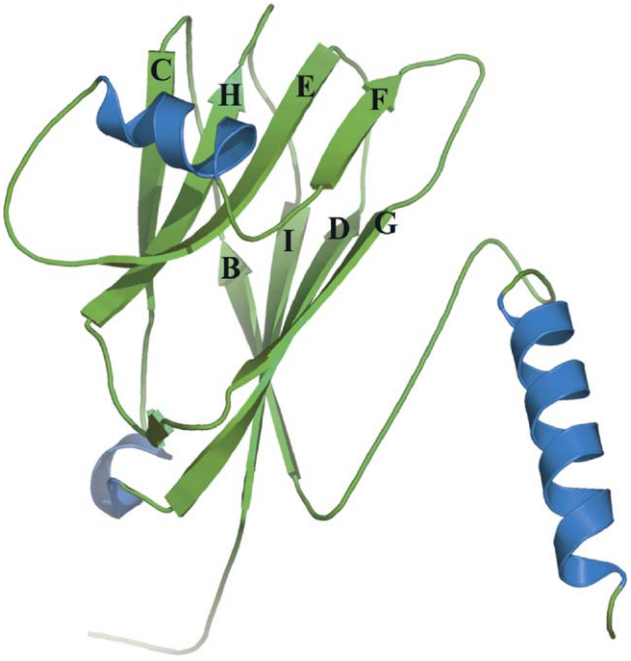

Fig. 2. Ribbon image of the B subunit of R-CMV CP model with sheets and helices of interests labelled. Sheet labelling corresponds to TAV labelling of Lucas et al. [24]. Sheets are coloured green and helices are blue. This figure was rendered by PyMOL [25].

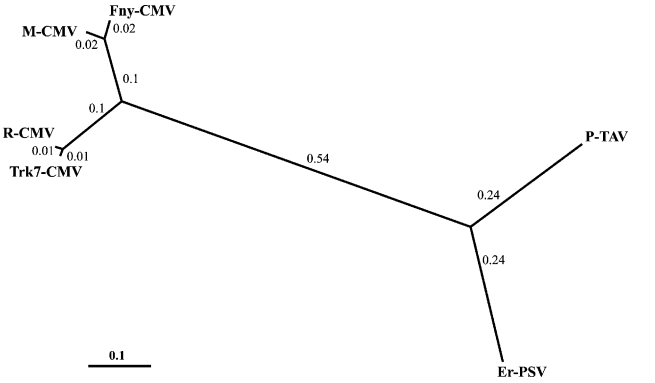

Fig. 3. Phylogenetic tree of the amino acid sequences of the studied *cucumovirus* CPs using PROTDIST and KITSCH programs. The values at the forks indicate branch lengths determined with the Fitch–Margoliash method. The scale bar shows the number of substitutions per residue.

assembled virus capsid because it is located on the surface and is well accessible.

In case of the other cucumovirus CPs studied, Ala, Ala, Val and Thr residues are at position 193 in Fny, M-CMV, P-TAV and Er-PSV CP, respectively (Fig. 1). Er-PSV would cause stunting symptoms only if this amino acid were responsible for evolving this symptom, but because of the high level of the sequential difference other symptom determinants are also present, therefore stunting attaining is not probable.

3.3. The role of the residues 129 and 214 in squash infection

The M strain of CMV does not infect squash plants systemically, while Fny-CMV causes very strong symptoms in this plant [20]. In the reference publication, the authors verified that the residues at positions 129 and 214 of CP determine the evolving symptoms. At this position M and Fny-CMV CP contain leucine and an arginine, respectively. Furthermore, proline and glycine are found at positions 129 and 214, respectively. Altogether six mutations were created and the following experimental results were obtained (Table 3): in M-CMV CP, the L129P mutation caused chlorotic lesions 6–9 days post-inoculation (d.p.i.), the R214G mutation led to stunting and chlorotic lesions 6–9 d.p.i. and the L129P/R214G double mutant variant caused severe stunting and mosaic symptoms 3–4 d.p.i. For variants of Fny-CMV CP: the P129L mutant abolishes infection, the G214R variant causes stunting and chlorotic symptoms 6–9 d.p.i. and the P129L/G214R double mutant also abolished the infection.

Residue 129 is the first unit of the βE–αEF loop (129–136), which is located between the E β-sheet and the EF α-helix (Fig. 7). This amino acid is on the external surface of the assembled virus particle. Residue 214 is on the C-terminal tail of the CP which is on the internal surface of the virus capsid therefore probably participates in the infection process as a single macromolecule. In this case, it is more complicated to find a connection between the evolving symptoms and the structural characteristics.

Mutations L129P and P129L in the M and Fny-CMV CP: near residue 129 there is a protein kinase C recognition site

Table 3
Systemic infection of squash by M-CMV, Fny-CMV [20] and their various CP mutants related to structural characteristics

CP variants	Systemic symptoms[a]	PKC phosphorylation site at the positions 212–214[b]	Flexibility of the βE–αEF loop[b]
M native	None	Yes	Flexible
M-L129P	Chll.	Yes	Rigid
M-R214G	St.; Chll.	No	Flexible
M-L129P/R214G	Sev. St.; Mos.	No	Rigid
Fny native	Sev. St.; Mos.	No	Rigid
Fny-P129L	None	No	Flexible
Fny-G214R	St.; Chll.	Yes	Rigid
Fny-P129L/G214R	None	Yes	Flexible

[a] Sev.: severe; St.: stunting; Mos.: green–yellow mosaic; Chll.: chlorotic lesions.
[b] Based on PROSITE functional site search and structure analysis.

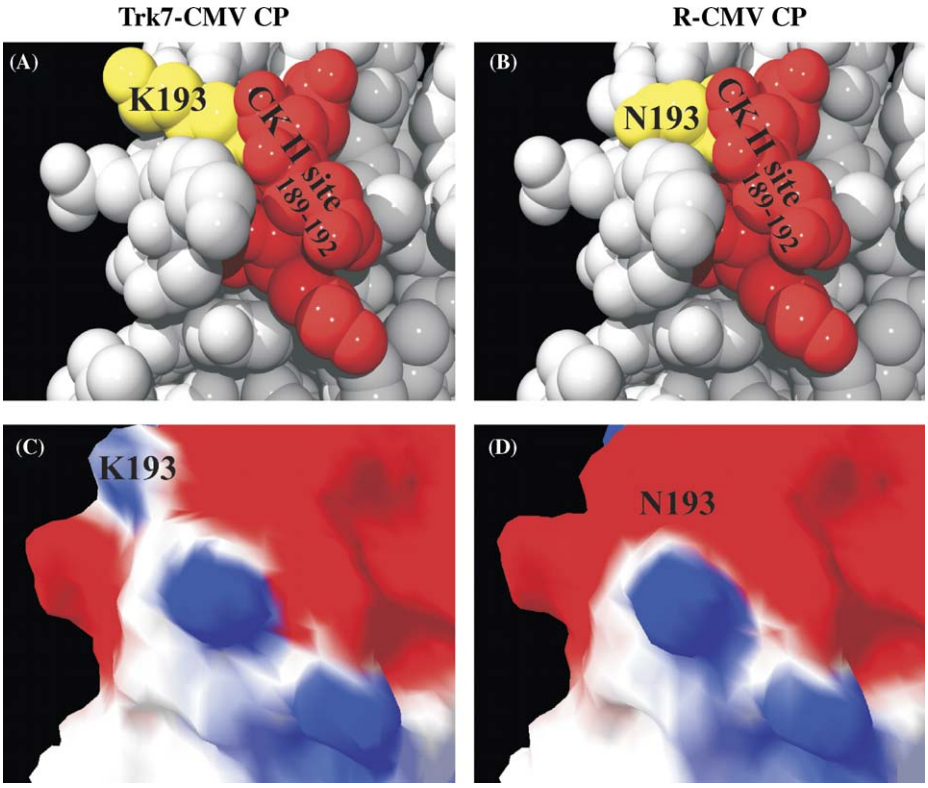

Fig. 4. Analysis of the Trk7 and R-CMV CP structures at position 193. (A and B) van der Waals surface representations of Trk7 and R-CMV CP, respectively. Residue 193 and CK II kinase site are indicated. (C and D) Electrostatic potential surface representation of Trk7 and R-CMV CP from the same view. Red, regions with potential less than −1.8 kT; white, 0.0; blue, greater than +1.8 kT. (A and B) Rendered by the POV-Ray 3.5 program.

(residues 124–126), but no significant electrostatic potential differences were recognized between the two CPs (Fig. 5), though leucine is larger and more hydrophobic, than proline. A possible interpretation is that the flexibility of the βE–αEF loop starting at the position 129 depends on the quality of this amino acid, since leucine allows more flexible loop conformations than the rigid proline. Thus, we conclude that the loop starting with a proline residue is allows to develop the infection function.

Mutations R214G and G214R in the M and Fny-CMV CP result in the partial charge of the electrostatic potential from positive to neutral and vice versa, especially if an arginine is located at the position 214, a PKC phosphorylation site will develop here (S212-T213-R214). From this, we can draw the conclusion that the phosphorylation of this site inhibits infection.

In the case of L129P/R214G double mutation in the M-CMV CP the βE–αEF loop is rigid and there is no phosphorylation site present at the position 214, thus both mutations amplifying their effects cause severe symptoms in the host plant. The double mutation P129L/G214R in the Fny-CMV CP makes the βE–αEF loop flexible, so phosphorylation can occur around position 214. Accordingly both mutations weaken their effects and entirely abolish the possibility of the infection.

Interestingly, in the R214G mutant of M-CMV and the P129L mutant of Fny-CMV CPs there are no phosphorylation sites at positions 212–214 and the βE–αEF loop is flexible (Table 3). Nevertheless, the mutated M-CMV CP causes stunting and chlorotic lesions, while the mutant of the Fny-CMV CP is non-infectious. Consequently, in Fny-CMV increase of flexibility of the βE–αEF loop results in the loss of infectivity, while in M-CMV, where originally the βE–αEF loop is flexible not allowing phosphorylation, the virus already becomes infectious.

We can conclude that phosphorylation at sites 212–214 and the flexible βE–αEF loop amplifying their effects contribute to inhibition of the infection. Inspection of other modelled cucumovirus CPs indicates that the sequence of the βE–αEF loop is remarkably conservative. The R, Trk7-CMV and Er-PSV CPs also contain proline at position 129, but there is an aspartate in the P-TAV CP at this site. We can make predictions for the other cucumoviruses on the basis of the previous considerations however, the reality is more complicated. Due to the presence of a proline residue the βE–αEF loop flexibility is low in case of R, Trk7-CMV and Er-PSV CP and there is no PKC phosphorylation site present near position 212, therefore these viruses will probably infect the squash plant. The βE–αEF loop is flexible in P-TAV but there is no PKC phosphorylation site at positions 212–214; therefore, we cannot decide whether it infects the squash plant or not.

3.4. Positions 129 and 162 are important for maize infection

Maize shows resistance against M-CMV, while it is infected by the Fny strain of CMV. Solely the CP is responsible for the

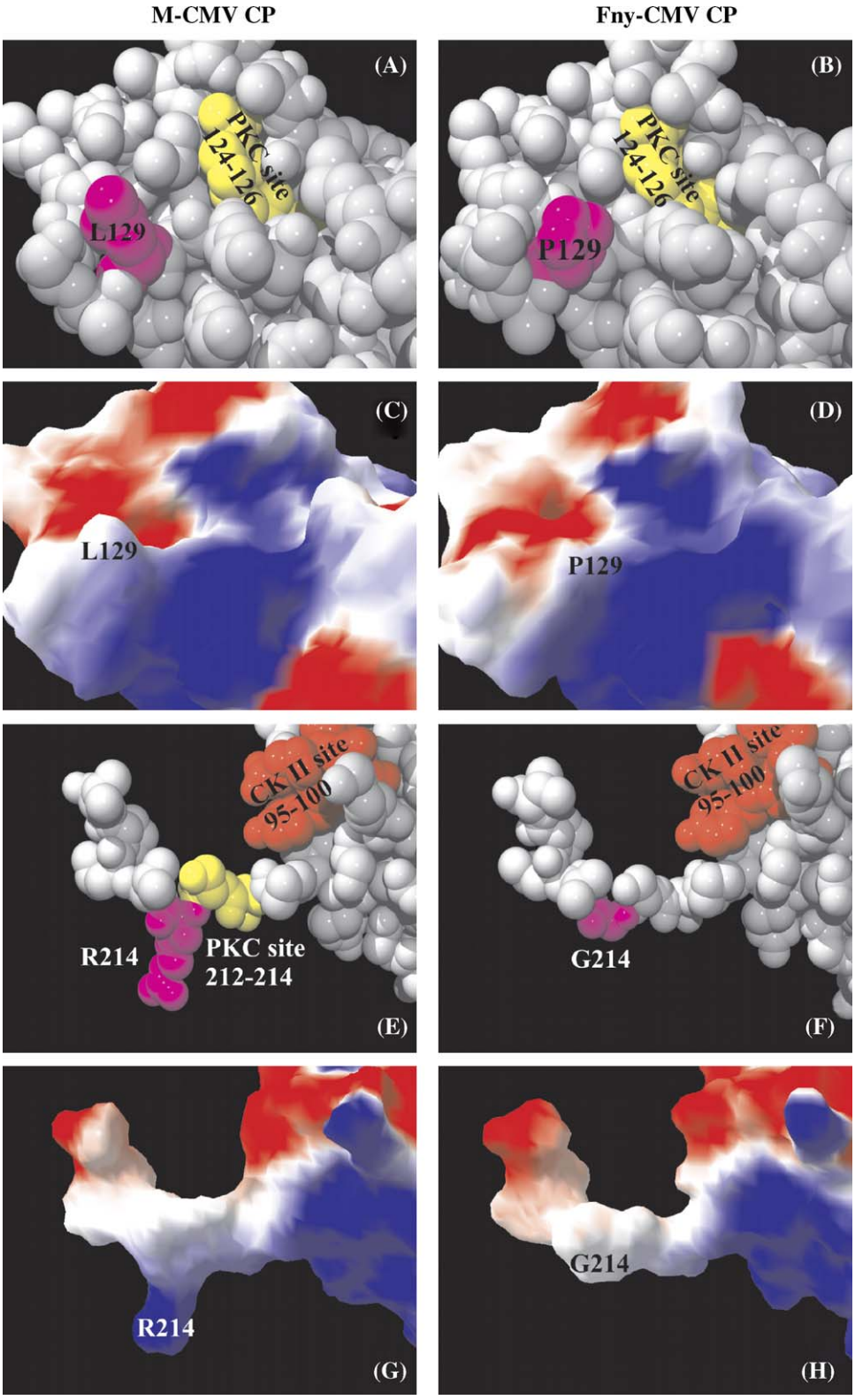

Fig. 5. Analysis of the M and Fny-CMV CP structures at positions 129 and 214. (A and B; E and F) van der Waals surface representations of M and Fny-CMV CP, respectively. Residues 129, 214 and kinase recognition sites are indicated. (C and D; G and F) Electrostatic potential surface representation of M and Fny-CMV CP. Red, regions with potential less than −1.8 kT; white, 0.0; blue, greater than +1.8 kT.

evolving symptoms, as it was verified in the reference [21]. Changes in the CP of M-CMV at both positions 129 and 162 are required to overcome the resistance against M-CMV in maize. Three single point mutations in the M-CMC CP were created [21]: L129P, T162A and C168Y, two double mutations: L129P/T162A and L129P/C168Y, as well as one triple mutation: L129P/T162A/C168Y. None of the single mutants cause symptoms and one of the double mutants (L129P/C168Y) is

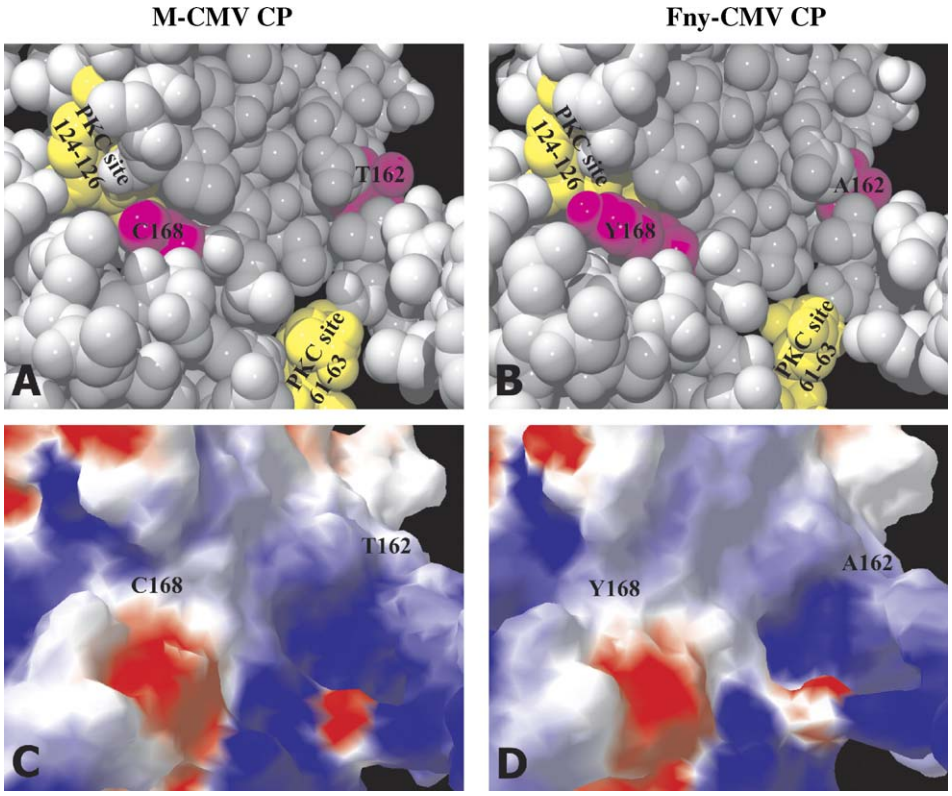

Fig. 6. Analysis of the M and Fny-CMV CP structures at positions 162 and 168. (A and B) van der Waals surface representations of M and Fny-CMV CP, respectively. Residues 162, 168 and PKC recognition sites are indicated. (C and D) Electrostatic potential surface representation of M and Fny-CMV CP. Red, regions with potential less than −1.8 kT; white, 0.0; blue, greater than +1.8 kT.

also unable to infect. Only the L129P/T162A double mutant and the triple mutant proved to be infectious.

Detailed discussion on the role of the P129 mutant is described above (Fig. 5A–D). On the basis of experimental data similar conclusions can be drawn in this case, too. We found that the residues 162 and 168 are on the surface of the CP and they are located on the inner surface of the assembled virus particle. Significant electrostatic potential differences were not recognized around these residues (Fig. 6). Unfortunately, a PROSITE search did not predict any phosphorylation site at the position 162 or 168. However, T162 and Y168 can be phosphorylated, so it seems that the phosphorylation state of the CP influences the cell-to-cell movement of the virus. Interestingly, in the 3D model the predicted PKC phosphorylation site (124–126) is located spatially very close to residue 168.

In the L129P mutant, the βE–αEF loop has a low flexibility, however T162 can and C168 cannot be phosphorylated, respectively (Table 4). In case of the T162A mutant, no phosphorylation is possible at positions 162 and 168, while the βE–αEF loop is flexible due to the presence of the residue L129. In the C168Y mutant, both the T162 and the Y168 residues can be phosphorylated, but the βE–αEF loop is flexible. In case of the infectious L129P/T162A double mutation the βE–αEF loop has a low flexibility and the A162 and C168 residues cannot be phosphorylated. The βE–αEF loop also has a low flexibility and the T162 and Y168 residues are capable to bind a phosphate group in the L129P/C168Y double mutant. Finally, in case of the infectious triple mutant L129P/T162A/C168Y, the βE–αEF loop is rigid and the A162 residue cannot be phosphorylated, while the Y168 residue can.

Summarizing these observations the rigidity of the βE–αEF loop is necessary but not sufficient for developing infection. Phosphorylation at position 162 abolishes the infection but the phosphorylation state of position 168 does not influence the infectivity. Extrapolating this conclusion the following predictions can be made for the other studied CP models: R-CMV (P129, A162 and Y168) and Trk7-CMV (P129, A162 and Y168) probably infect maize, while it is unlikely, that P-TAV (D129, P162 and F168) is infectious.

3.5. Some remarks for the aphid vector transmission

As it has been verified experimentally the βH–βI loop [22] and the βE–αEF loop [23] have a major role in the aphid vector transmission of the virus. According to our hypothesis, the βH–βI loop has dual function, it works partly as a recognition epitope in the aphid vector transmission, and partly as a phosphorylation site (residues 189–192, CK II) participating in the host response. Nine CP mutants were created (D191A, D191K, D192A, D192K, L194A, E195A, E195K, D197A and D197K) from the Fny-CMV CP and discussed in the light of aphid vector transmission [22]. Eight of the nine mutants were defective in aphid vector transmission, but all of them were infectious and showed several symptoms. Different symptoms

Table 4
Systemic infection of maize by M-CMV, Fny-CMV and their various CP mutants [21] and its theoretical background

CP variants	Systemic symptoms[a]	Possible phosphorylation at position[b]		Flexibility of the βE–αEF loop[b]
		162	168	
M native	None	Yes	No	Flexible
M-L129P	None	Yes	No	Rigid
M-T162A	None	No	No	Flexible
M-C168Y	None	Yes	Yes	Flexible
M-L129P/T162A	Chls. and Ncrs.	No	No	Rigid
M-L129P/C168Y	None	Yes	Yes	Rigid
M-L129P/T162A/C168Y	Chls. and Ncrs.	No	Yes	Rigid
Fny native	Chls. and Ncrs.	No	Yes	Rigid

[a] The foliar symptoms are varied from chlorotic streaks to necrotic streaks. Chls.: chlorotic streaks; Ncrs.: necrotic streaks.
[b] Based on PROSITE functional site search and structure analysis.

are appeared, because probably the recognition sequence of the phosphorylation site (189–192) was modified in case of mutations at positions 191 and 192.

4. Conclusions

During virus infection the plant tries to overcome the external biological attack with its own biochemical tools. In cases of cucumoviruses and plant viruses, phosphorylation of virus proteins may also play considerable role in the host response. In this paper, we discuss the published cytopathological determinants of the CP on the basis of theoretical considerations. In all cases, high flexibility of the βE–αEF loop is required to develop virus resistance (Fig. 7). Such straightforward conclusions cannot be drawn about the phosphorylation states. In the cases discussed here, phosphorylation of CP supports, or abolishes infectivity or it is indifferent. We suggest that in the examined cases, experimental study of phosphorylation states is required to have more detailed overlook on the molecular mechanism of the viral infection. Furthermore, it can be worth while to identify the host factors or proteins participating in the response. We believe that well targeted molecular biological experiments can be planned on the basis of this work. A few experiments are already in progress in our laboratory.

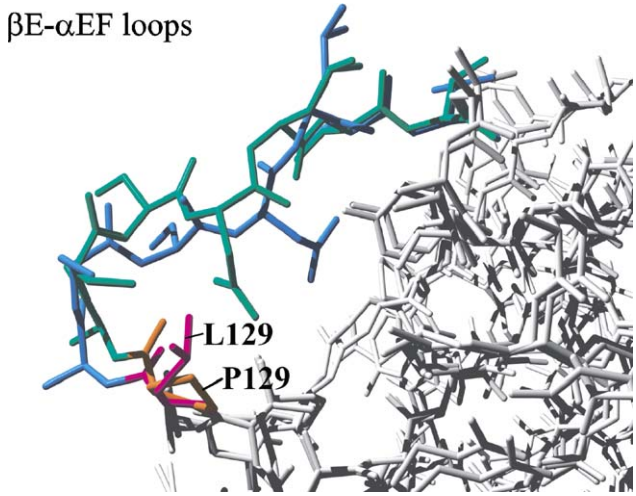

Fig. 7. Detailed structure representation of the βE–αEF loop conformations in Fny and M-CMV CP. Orange and pink indicate residue 129 in Fny and M-CMV CP, while green and blue indicate the βE–αEF loop structure in Fny and M-CMV CP, respectively. This figure was rendered by the POV-Ray 3.5 program.

Acknowledgements

The work was supported by the National Foundation for Scientific Research (OTKA) Science School TS 447778 and VRTP IMPACT QLK3-CT-2000-00361. K. Salánki is recipient of a Bólyai János Fellowship from the Hungarian Academy of Sciences.

References

[1] T.J. Smith, E. Chase, T. Schmidt, K.L. Perry, The structure of Cucumber mosaic virus and comparison to Cowpea chlorotic mottle virus, J. Virol. 74 (2000) 7578–7586.
[2] P. Palukaitis, F. García-Arenal, Cucumoviruses, Adv. Virus Res. 62 (2004) 241–323.
[3] M. Suzuki, S. Kuwata, J. Kataoka, C. Masuta, N. Nitta, Y. Takanami, Functional analysis of deletion mutants of cucumber mosaic virus RNA3 using an in vitro transcription system, Virology 183 (1991) 106–113.
[4] I.B. Kaplan, L. Zhang, P. Palukaitis, Characterization of cucumber mosaic virus. V. Cell-to-cell movement requires capsid protein but not virions, Virology 246 (1998) 221–231.
[5] H. Nagano, K. Mise, I. Furusawa, T. Okuno, Conversion in the requirement of coat protein in cell-to-cell movement mediated by the cucumber mosaic virus movement protein, J. Virol. 75 (2001) 8045–8053.
[6] K. Salánki, Á. Gellért, E. Huppert, G. Náray-Szabó, E. Balázs, Compatibility of the movement protein and the coat protein of cucumoviruses is required for cell-to-cell movement, J. Gen. Virol. 85 (2004) 1039–1048.
[7] L. Terradot, M. Souchet, D.G. Ducray-Bourdin, Analysis of three-dimensional structure of *Potato leafroll virus* coat protein obtained by homology modelling, Virology 286 (2001) 72–82.
[8] G. Náray-Szabó, Analysis of molecular recognition: steric electrostatic and hydrophobic complementarity, J. Mol. Recog. 6 (1993) 205–210.
[9] S.B. Needleman, C.D.A. Wunsch, general method applicable to the search for similarities in the amino acid sequence of two proteins, J. Mol. Biol. 48 (1970) 443–453.
[10] GCG, Wisconsin Package, version 10.0, Accelrys Inc, San Diego, CA, 1999.
[11] J. Felsenstein, PHYLIP, version 3.5, University of Washington, Seattle, WA, 1998.
[12] A. Sali, Modeling mutations and homologous proteins, Curr. Opin. Biotechnol. 6 (1995) 437–451.

[13] S.J. Weiner, P.A. Kollman, D.A. Case, U.C. Singh, C. Ghio, G. Alagona, S. Profeta, P. Weiner, A new force field for molecular mechanical simulation of nucleic acids and proteins, J. Am. Chem. Soc. 106 (1984) 765–784.
[14] M.K. Gilson, K.A. Sharp, B. Honig, Calculating electrostatic interactions in biomolecules: method and error assessment, J. Comp. Chem. 9 (1987) 327–335.
[15] A. Nicholls, K. Sharp, B. Honig, Protein folding and association—insights from the interfacial and thermodynamic properties of hydrocarbons, Proteins Struct. Funct. Genet. 11 (1991) 281–296.
[16] N. Guex, M.C. Peitsch, SWISS-MODEL and the Swiss-PdbViewer: an environment for comparative protein modelling, Electrophoresis 18 (1997) 2714–2723.
[17] R.A. Laskowski, M.W. MacArthur, D.S. Moss, J.M. Thornton, PROCHECK: a program to check the stereochemical quality of protein structures, J. Appl. Cryst. 26 (1993) 283–291.
[18] C.J. Sigrist, L. Cerutti, N. Hulo, A. Gattiker, L. Falquet, M. Pagni, A. Bairoch, P. Bucher, PROSITE: a documented database using patterns and profiles as motif descriptors, Brief Bioinf. 3 (2002) 265–274, http://us.expasy.org/prosite.
[19] D. Szilassy, K. Salánki, E. Balázs, Stunting induced by Cucumber mosaic cucumovirus-infected *Nicotiana glutinosa* is determined by a single amino acid residue in the coat protein, MPMI 12 (1999) 1105–1113.
[20] S.M. Wong, S.S.C. Thio, M.H. Shintaku, P. Palukaitis, The rate of cell-to-cell movement in squash of cucumber mosaic virus is affected by sequences of the capsid protein, MPMI 12 (1999) 629–632.
[21] K.H. Ryu, C.H. Kim, P. Palukaitis, The coat protein of cucumber mosaic virus is a host range determinant for infection of maize, MPMI 11 (1998) 351–357.
[22] S. Liu, X. He, G. Park, C. Josefsson, K.L. Perry, A conserved capsid protein surface domain of cucumber mosaic virus is essential for efficient aphid vector transmission, J. Virol. 76 (2002) 9756–9762.
[23] K.L. Perry, L. Zhang, M.H. Shintaku, P. Palukaitis, Mapping determinants in Cucumber mosaic virus for transmission by *Aphis gossypii*, Virology 205 (1994) 591–595.
[24] R.W. Lucas, S.B. Larson, M.A. Canady, A. McPherson, The structure of tomato aspermy virus by X-ray crystallography, J. Struct. Biol. 139 (2002) 90–102.
[25] PyMol, version 0.97, DeLano Scientific, San Carlos, CA, 2002.